

Numerical equality tests for rational maps and signatures of curves

Timothy Duff

tduff3@gatech.edu

School of Mathematics, Georgia Tech
Atlanta, Georgia, USA

Michael Ruddy

michael.ruddy@mis.mpg.de

Max Planck Institute for Mathematics in the Sciences
Leipzig, Germany

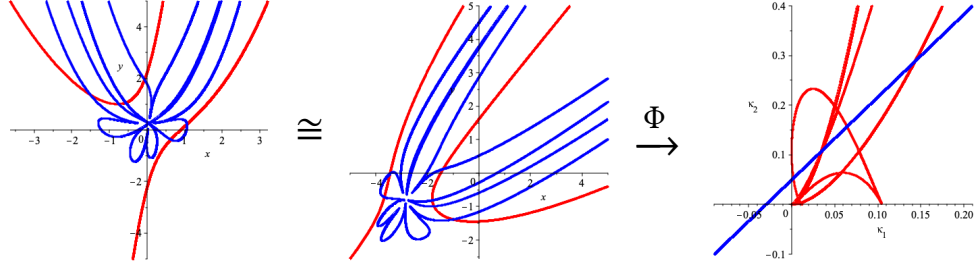


Figure 1: Two curves and their signature in red. A line and its pullback in blue.

ABSTRACT

We apply numerical algebraic geometry to the invariant-theoretic problem of detecting symmetries between two plane algebraic curves. We describe an efficient equality test which determines, with “probability-one”, whether or not two rational maps have the same image up to Zariski closure. The application to invariant theory is based on the construction of suitable signature maps associated to a group acting linearly on the respective curves. We consider two versions of this construction: differential and joint signature maps. In our examples and computational experiments, we focus on the complex Euclidean group, and introduce an algebraic joint signature that we prove determines equivalence of curves under this action. We demonstrate that the test is efficient and use it to empirically compare the sensitivity of differential and joint signatures to noise.

KEYWORDS

differential invariants, invariant theory, numerical algebraic geometry, polynomial systems, Euclidean group, computer algebra, homotopy continuation

1 INTRODUCTION

This paper studies two related problems.

Problem 1. Given two irreducible algebraic varieties, $X_0 \subset \mathbb{C}^{n_0}$ and $X_1 \subset \mathbb{C}^{n_1}$, and two rational maps, $\Phi_0 : X_0 \dashrightarrow \mathbb{C}^m$ and $\Phi_1 : X_1 \dashrightarrow \mathbb{C}^m$, decide if $\overline{\text{im } \Phi_0} = \overline{\text{im } \Phi_1}$.

Problem 2. Given a positive dimensional algebraic group $G \subset \text{PGL}_3(\mathbb{C})$ acting linearly on \mathbb{C}^2 and two plane algebraic curves $C_0, C_1 \subset \mathbb{C}^2$, decide if there exists $g \in G$ such that $C_0 = g \cdot C_1$.

In the context of *differential invariant theory*, we can reduce Problem 2 to Problem 1 by constructing a suitable *signature map* for the action of G on the curves C_1, C_2 . For Problem 1, the field of

numerical algebraic geometry furnishes a suite of “probability-one” tests. In this article, we explain the aforementioned approaches to these problems in detail and demonstrate that they yield practical *equality tests* for both problems.

In Problem 1, $\overline{\text{im } \Phi_i}$ denotes the Zariski closure of the image of Φ_i . We do not address the more delicate problem of deciding equality of the constructible sets $\text{im } \Phi_i$.

A formally correct algorithmic solution to Problem 1 clearly depends on how the input is “given” to us and what type of guarantee we seek. A natural route via symbolic computation is to compute the ideal of implicit equations for each map and check if these ideals are equal. This is a standard application of Gröbner bases; resultants and more specialized techniques may provide useful alternatives.

Our approach to Problem 1 via numerical algebraic geometry is in the same spirit as previous works [8, 17, 18], where the cost of implicitization is replaced by the cost of computing certain *witness sets*. A key feature of our approach is that it requires a pre-computed witness set for only one of the maps, say Φ_1 . This feature is motivated mainly by our interest in Problem 2. We view computing a witness set for Φ_1 as an *offline* cost. The *online* cost of testing equality via Algorithm 1 is typically negligible by comparison. This is advantageous in a scenario where we wish to test Φ_1 against many different choices of Φ_0 .

To reduce Problem 2 to Problem 1, one may use the maps obtained by restricting a pair of independent, rational differential invariants for G to C_0 and C_1 [22], which can be explicitly constructed via the Fels-Olver moving frame method [11] or its algebraic formulation [20]. The image of an algebraic curve C under this map is the curve’s *differential signature*. In greater generality, differential signatures may be constructed for smooth submanifolds of some ambient space equipped with a Lie group action. The differential signature locally characterizes the manifold’s equivalence class under the action, meaning that manifolds with the same signature are locally equivalent under the Lie group [11]. For an algebraic group

acting on \mathbb{C}^2 and a plane curve $C \subset \mathbb{C}^2$, such a construction yields a rational map $\Phi : \mathbb{C}^2 \dashrightarrow \mathbb{C}^2$. In this special case, local equivalence implies global equivalence.

Example 1.1. In Figure 1, the red curve on left depicts real points (x, y) such that $8x^3 - 20xy + 2y^2 + 5x - 10 = 0$. Applying a real rotation and translation yields the curve in the middle. Thus these curves are equivalent under the linear action of the complex Euclidean group $\mathcal{E}_2(\mathbb{C})$. The closed image of their respective differential signature maps is the red curve of degree 48 depicted on the right.

Differential signatures of curves have been successfully applied to object recognition under noise, with applications ranging from jigsaw puzzle reconstruction [19] to medical imaging [13]. Differential signatures have also been used to solve classical invariant theory problems such as determining equivalence of binary and ternary forms [4, 21, 29]. The setting of algebraic curves is a useful testing ground for algorithms in this subject. In [7] the notion of a signature polynomial was introduced to determine equivalence of plane algebraic curves via implicitization methods. In [22] it is shown that this reduction to implicitization can always be done for any group acting as in Problem 2.

In this paper we show that the numerical algorithm for Problem 1 yields an effective way for solving Problem 2 using differential signatures, even when implicitization is not practically feasible. We also consider *joint signatures*, which are obtained by constructing rational maps using joint invariants of the induced action of G on the product $\mathbb{C}^2 \times \dots \times \mathbb{C}^2$ [30]. While we focus on plane curves, in principle the numerical equality test can be used to determine equivalence of higher dimensional varieties through differential or joint signatures, provided one can find a suitable set of *rational* differential or joint invariants.

In Section 2, we review notions from numerical algebraic geometry and describe a general solution to Problem 1 (Algorithm 1.) Section 3 considers the signature approach to Problem 2. In 3.1 we follow the construction in [7, 22] to describe a differential signature for plane algebraic curves using a *classifying pair* of differential invariants. In 3.2 we describe how joint signatures can be used to determine equivalence of plane curves using lower order differential invariant functions, with a detailed analysis in the case of the complex Euclidean group $\mathcal{E}_2(\mathbb{C})$. In Section 4, we describe an implementation in Macaulay2 [12], which has been successful for studying both classes of maps on curves of degree up to 10. Our (reproducible) experiments show that offline witness computation for plane curves of various degrees is feasible, that the online equality test gives a fast alternative to symbolic methods, and that the numerical approach is robust in a certain regime of noise.¹

2 NUMERICAL EQUALITY

2.1 Background

In this subsection we fix notation and terminology related to algebraic varieties and witness sets. A more comprehensive overview of numerical algebraic geometry may be found in the survey [32] or books [3, 33]. A general system of polynomial equations is denoted by a c -tuple $f = (f_1, \dots, f_c)$ for $f_1, \dots, f_c \in \mathbb{C}[x_1, \dots, x_n]$. Where

convenient, we may identify f with a map $\mathbb{C}^n \rightarrow \mathbb{C}^c$. The vanishing locus $V(f) := \{x \in \mathbb{C}^n \mid f_1(x) = \dots = f_c(x) = 0\}$ is a closed subvariety of \mathbb{C}^n . If c is the codimension of $V(f)$, then f is said to be a *regular sequence* and the variety $V(f)$ is a *complete intersection*. For polynomial systems $f = (f_1, \dots, f_k)$ and $g = (g_1, \dots, g_{k'})$ we write $(f \mid g) := (f_1, \dots, f_k, g_1, \dots, g_{k'})$, yielding a polynomial system whose vanishing locus is $V(f) \cap V(g)$. A property is said to hold generically on an irreducible variety X if it holds on some nonempty Zariski-open $U \subset X$. We say that f is *generically reduced* along X if there exists a point $x \in X$ such that the tangent space $T_x(f) = \ker(df_i/dx_j)$ has dimension $n - c$.

The main data structures in numerical algebraic geometry are variations on the notion of a *witness set*. The overarching idea is to represent an irreducible variety $X \subset \mathbb{C}^n$ by its intersection with a generic affine linear subspace of complementary dimension. The number of points in such an intersection is the degree, $\deg X$.

We define a c -slice in \mathbb{C}^n to be a polynomial system consisting of c affine hyperplanes, $L = (l_1, \dots, l_c)$ with $l_i \in \mathbb{C}[x_1, \dots, x_n]_{\leq 1}$. For convenience we write L in place of $V(L(x))$ and also use the notation L^c . For X an irreducible variety of codimension c and a generic slice L^c , the intersection $X \cap L^c$ is *transverse*, consisting of $\deg X$ isolated, nonsingular points.

The standard definition of a witness set for a variety assumes that defining equations for the variety of interest are known. A more flexible notion is that of a *pseudo-witness set* for a rational map. This was first studied for linear projections in [17]. Our Definition 2.1 differs from that used in [3, 17, 18]; to distinguish our setup, we provisionally use the term *weak pseudowitness set*.

Definition 2.1. Let $V(f) \subset \mathbb{C}^n$ be Zariski-closed, $X \subset V(f)$ be one of its irreducible components, and $\Phi : X \dashrightarrow \mathbb{C}^m$ be a rational map. Set $c = \text{codim } V(f)$, $d = \dim \text{im } \Phi$. A weak pseudowitness set for Φ is a quadruple $(f, \Phi, (L|L'), \{w_1, \dots, w_e\})$, where L is a generic affine $(m - d)$ -slice of $\text{im } \Phi$, L' is a generic affine $(c - m + d)$ -slice of X , and such that w_1, \dots, w_e are points in $X \cap L'$ where Φ is defined such that $\text{im } \Phi \cap L = \{\Phi(w_1), \dots, \Phi(w_e)\}$ and $e = \deg \text{im } \Phi$.

The data in Definition 2.1 are already sufficient for testing queries of the form $y \in \text{im } \Phi$, as noted in [17, Remark 2]. For testing, $y \in \text{im } \Phi$ and other applications, the stronger notion is required [18]. Further applications of pseudowitness sets are in [6, 8].

In our context, equations defining $\text{im } \Phi$ are seldom known, so in what follows we may informally refer to the objects of Definition 2.1 and their multiprojective counterparts in Definition 2.2 as “witness sets” without ambiguity.

Following [15, 16, 25], we give a multiprojective generalization of Definition 2.1. For irreducible $X \subset \mathbb{C}^n$, we fix (n_1, \dots, n_k) , an integer partition of n , and consider X in the affine space $\mathbb{C}^{n_1} \times \dots \times \mathbb{C}^{n_k}$. We consider slices $L^e = L^{e_1} \mid \dots \mid L^{e_k}$, where $e = (e_1, \dots, e_k) \in \mathbb{N}^k$ is an integral vector such that $e_1 + \dots + e_k = \dim X$, and L^{e_j} is a e_j -slice consisting of e_j affine hyperplanes in the coordinates of \mathbb{C}^{n_j} . We say that e is a *multidimension* of X if for generic L^e the intersection $X \cap L^e$ is a finite set of nonsingular points; the number of points for such L^e is a constant called the *e -multidegree* $\deg_e X$.

Definition 2.2. Let f, X, c, L', Φ be as in 2.1, and e be a multidimension of $\text{im } \Phi$ corresponding to some partition of n . An e -weak

¹Obtain the code at <https://github.com/timduff35/NumericalSignatures>.

pseudowitness set for Φ consists of $(f, \Phi, (L^e|L'), \{w_1, \dots, w_e\})$, such that $\overline{\text{im } \Phi} \cap L^e = \{\Phi(w_1), \dots, \Phi(w_e)\}$ and $e = \deg_e \overline{\text{im } \Phi}$.

The general membership test for multiprojective varieties proposed in [16] uses the stronger notion of a witness collection. This is required since for an arbitrary point $x \in X$ there may not exist transverse slices $L^e \ni x$ for e ranging over all multidimensions of X —see [16, Example 3.1]. This subtlety is not encountered for generic $x \in X$; we record this basic fact in Proposition 2.3.

PROPOSITION 2.3. *Fix irreducible $X \subset \mathbb{C}^{n_1} \times \dots \times \mathbb{C}^{n_k}$ and e some multi-dimension of X . For $x = (x_1, \dots, x_k) \in X$ generic, there exists an e -slice $L^e \ni x$ such that $\dim(X \cap L^e) = 0$. Moreover, for $x \notin X_{\text{sing}}$, we also have that $x \notin (X \cap L^e)_{\text{sing}}$ for generic L^e .*

PROOF. For generic x_1 in the image of $\pi_1 : X \rightarrow \mathbb{C}^{n_1}$ we have that the fiber $\pi_1^{-1}(x_1)$ has dimension $\dim X - \dim \pi_1(X)$. Choose such an x_1 and let $L^{e_1} \ni x_1$ be generic so that $\pi_1(X) \cap L^{e_1}$ has dimension $\dim \pi_1(X) - e_1$. It follows that $(X \cap L^{e_1})$ has dimension $\dim X - e_1$. This construction holds for all x_1 on some Zariski open $U_1 \subset \pi_1(X)$. Repeating this construction for the remaining factors yields U_2, \dots, U_k such that the first part holds for all $x \in U_1 \times \dots \times U_k$. The second part follows from the appropriate Bertini theorem, cf. [14, Thm 17.16]. \square

2.2 A general equality test

Now let $\Phi_0 : X_0 \dashrightarrow \mathbb{C}^m$ and $\Phi_1 : X_1 \dashrightarrow \mathbb{C}^m$ denote two rational maps with each $X_i \subset \mathbb{C}^{n_i}$ of codimension c_i . Problem 1 from the introduction asks us to decide whether or not their images are equal up to Zariski closure. A probabilistic procedure is given in Algorithm 1. This equality test refines general membership and equality tests from numerical algebraic geometry, which are summarized in [33, Ch. 13, 15] and [3, Ch. 8, 16]. Our setup is motivated by an efficient solution to Problem 2. Following the standard terminology, our test correctly decides equality with “probability-one” in an idealized model of computation. This is the content of Theorem 2.4. Standard disclaimers apply, since any implementation must rely on numerical approximations in floating-point [3, Ch. 3, pp. 43–45].

Algorithm 1 assumes different representations for the two maps. The map Φ_1 is represented by a witness set in the sense of Definition 2.1, say $(f_1, \Phi_1, (L_1|L'_1), \{w_1, \dots, w_e\})$. In fact, the only data needed by Algorithm 1 are the map itself Φ_1 , the slice L_1 , and the points w_1, \dots, w_e . For the map Φ_0 , we need only a sampling oracle that produces generic points on X_0 and $\text{codim}(X_0)$ -many reduced equations vanishing on X_0 .

Suppose $\dim \overline{\text{im } \Phi_0} = \dim \overline{\text{im } \Phi_1} = d$. There is a probabilistic membership test for queries of the form $\Phi_0(x_0) \in \overline{\text{im } \Phi_1}$ based on homotopy continuation. The relevant homotopy depends parametrically on L_1 , a $(m-d)$ -slice $L_0 \ni \Phi_0(x_0)$, a (c_0-m+d) -slice $L'_0 \ni x_0$, and a regular sequence $f_0 = (f_{0,1}, \dots, f_{0,c_0})$ which is generically reduced with respect to X_0 . The homotopy H is defined as

$$H(x; t) = (f_0|L'_0|tL_1 \circ \Phi_0 + (1-t)L_0 \circ \Phi_0)(x). \quad (1)$$

In simple terms, H moves a slice through $\Phi_0(x_0)$ to the slice witnessing $\overline{\text{im } \Phi_1}$ as t goes from 0 to 1. A solution curve associated to (1) is a smooth map $x : [0, 1] \rightarrow \mathbb{C}^n$ such that $H(x(t), t) = 0$ for all t . For generic parameters L_0, L_1, L'_0 the Jacobian $H_x(x, t)$ is

invertible for all $t \in [0, 1]$, solution curves satisfy the ODE

$$x'(t) = -H_x(x, t)^{-1} H_t(x, t),$$

and each of the points w_1, \dots, w_e is the endpoint of some solution curve x with $x(0) \in X \cap L'_0$. These statements follow from more general results on *coefficient-parameter homotopy*, as presented in [27] or [33, Thm 7.1.1]. We assume a subroutine $\text{TRACK}(H, x_0)$ which returns $x(1)$ for the solution curve based at x_0 . In practice, the curve $x(t)$ is approximated by numerical predictor/corrector methods [1, 26]. We allow our TRACK routine to fail; this will occur, for instance, when $\Phi_0(x_0)$ is a singular point on $\overline{\text{im } \Phi_0}$. However, it will succeed for generic (and hence *almost all*) choices of parameters and $x_0 \in \mathbb{C}^{n_0}$. Algorithm 1 exploits this fact.

Algorithm 1. Probability-1 equality test

Input: Let $X_0 \subset \mathbb{C}^{n_0}, X_1 \subset \mathbb{C}^{n_1}$ be irreducible algebraic varieties, and $\Phi_0 : X_0 \rightarrow \mathbb{C}^m, \Phi_1 : X_1 \rightarrow \mathbb{C}^m$ be rational maps, represented via the following ingredients:

- 1) $(L_1, \{w_1, \dots, w_e\})$ with $\overline{\text{im } \Phi_1} \cap L_1 = \{\Phi_1(w_1), \dots, \Phi_1(w_e)\}$ and $e = \deg \overline{\text{im } \Phi_1}$ (cf. Definition 2.1),
- 2) $f_{0,1}, \dots, f_{0,c_0} \in \mathbb{C}[x_1, \dots, x_{n_0}]$: a generically reduced regular sequence such that $\text{codim}(X_0) = c_0$ and $X_0 \subset V(f_1, \dots, f_{c_0})$,
- 3) an oracle for sampling a point $x_0 \in X_0$, and
- 4) explicit rational functions representing each map Φ_i .

Output: YES if $\overline{\text{im } \Phi_0} = \overline{\text{im } \Phi_1}$ and NO if $\overline{\text{im } \Phi_0} \neq \overline{\text{im } \Phi_1}$.

- 1: sample $x_0 \in X_0$
- 2: $T_{x_0}(f) \leftarrow \ker(Df)_{x_0}$
- 3: $d \leftarrow \text{rank}(D\Phi_0)_{x_0}|_{T_{x_0}(f)}$
- 4: **if** $d \neq \dim \overline{\text{im } \Phi_1}$ **then return** NO
- 5: $H(x; t) \leftarrow$ the homotopy from equation 1
- 6: $x_1 \leftarrow \text{TRACK}(H, x_0)$
- 7: **if** $\Phi_0(x_1) \in \{\Phi_1(w_1), \dots, \Phi_1(w_e)\}$ **return** YES
- else return** NO

THEOREM 2.4. *For generic x_0, L_0, L'_0, L_1 , Algorithm 1 correctly decides if $\overline{\text{im } \Phi_0} = \overline{\text{im } \Phi_1}$.*

Remark 2.5. The set of “non-generic” L_1 depends on Φ_0 and Φ_1 . In practice, an oracle for sampling generic points could be provided by either a parametrization or by homotopy continuation with known equations for X_0 . The dimension $\dim \overline{\text{im } \Phi_1}$ is implicit in the description of the witness set.

PROOF. Since x_0 is generic and f_0 is generically reduced, we may assume that $d = \dim \overline{\text{im } \Phi_0}$. Noting line 4, we are done unless $d = \dim \overline{\text{im } \Phi_1}$. In this case, since the $\text{im } \Phi_i$ are irreducible,

$$\dim(\overline{\text{im } \Phi_0} \cap \overline{\text{im } \Phi_1}) = d \iff \overline{\text{im } \Phi_0} = \overline{\text{im } \Phi_1}. \quad (2)$$

As previously mentioned, generic slices give that the solution curve $x(t)$ associated to 1 with initial value x_0 exists and satisfies $x(t) \in V(f) \setminus V(f)_{\text{sing}}$ for all $t \in [0, 1]$. The endpoint x_1 is, *a priori*, a point of $V(f)$. Since $X_0 \setminus (X_0)_{\text{sing}}$ is a connected component of $V(f) \setminus V(f)_{\text{sing}}$ in the complex topology and $x_0 \in X_0$, so also must $x_1 \in X_0$. Hence $\Phi_0(x_1) \in \overline{\text{im } \Phi_0} \cap L_1$. Now if $\overline{\text{im } \Phi_0} = \overline{\text{im } \Phi_1}$, then clearly we must have

$$\Phi_0(x_1) \in \overline{\text{im } \Phi_1} \cap L_1 = \{\Phi_1(w_1), \dots, \Phi_1(w_e)\}, \quad (3)$$

as is tested on line 7. Conversely, if (3) holds, then

$$\dim(\overline{\text{im } \Phi_0} \cap \overline{\text{im } \Phi_1} \cap L_1) \geq 0,$$

which by (2) and the genericity of L_1 implies $\overline{\text{im } \Phi_0} = \overline{\text{im } \Phi_1}$. \square

In the multiprojective setting, we may give a similar argument, noting that Proposition 2.3 and genericity of $\Phi_0(x_0)$ are needed so that $H_X(x_0, 0)$ is invertible.

3 SIGNATURES OF CURVES

3.1 Differential signatures

In what follows, all plane curves are complex algebraic, irreducible, and of degree greater than one. Let $G \subset \mathcal{PGL}_3(\mathbb{C})$ be a positive dimensional algebraic group acting linearly on \mathbb{C}^2 with action $g \cdot (x, y) = (\bar{x}, \bar{y})$.

Definition 3.1. Two curves C_0, C_1 are said to be G -equivalent, denoted $C_0 \cong_G C_1$, if there exists a $g \in G$ such that $C_0 = g \cdot C_1$.

A differential signature that determines G -equivalence of curves can be constructed from a set of classifying invariants (Definition 3.6). We let J^n denote the n th order jet space, a complex vector space of dimension $(n+2)$ with coordinates $(x, y, y^{(1)}, \dots, y^{(n)})$. Letting $\Omega(J^n)$ denote the set of complex-differentiable functions from J^n to \mathbb{C} , the *total derivative operator* $\frac{d}{dx} : \Omega(J^n) \rightarrow \Omega(J^{n+1})$ is the unique \mathbb{C} -linear map satisfying the product rule and the relations $\frac{d}{dx}(x) = 1$, $\frac{d}{dx}(y^{(k)}) = y^{(k+1)}$ for $k \geq 0$, cf. [28, Ch. 7].

The *prolonged* action of G on J^n is given by

$$g \cdot (x, y, y^{(1)}, \dots, y^{(n)}) = (\bar{x}, \bar{y}, \bar{y}^{(1)}, \dots, \bar{y}^{(n)})$$

where

$$\begin{aligned} \bar{y}^{(1)} &= \frac{\frac{d}{dx} [\bar{y}(g, x, y)]}{\frac{d}{dx} [\bar{x}(g, x, y)]}, \\ \bar{y}^{(k+1)} &= \frac{\frac{d}{dx} [\bar{y}^{(k)}(g, x, y, y^{(1)}, \dots, y^{(k)})]}{\frac{d}{dx} [\bar{x}(g, x, y)]} \text{ for } k = 1, \dots, n-1. \end{aligned}$$

Definition 3.2. A *differential invariant* for the action of G is a function on J^n that is invariant under the prolonged action of G on J^n . The *order* of a differential invariant is the maximum k such that the function depends explicitly on $y^{(k)}$.

Definition 3.3. The n -th *jet* of an algebraic curve C is the image of the map $j_C^n : C \rightarrow J^n$ given (where defined) by

$$(x, y) \mapsto (x, y, y_C^{(1)}(x, y), y_C^{(2)}(x, y), \dots, y_C^{(n)}(x, y)),$$

where $y_C^{(k)}(x, y)$ is the k -th derivative of y with respect to x at the point $(x, y) \in C$.

The prolonged action of G is defined such that

$$g \cdot j_C^n(C) = j_{g \cdot C}^n(g \cdot C).$$

Definition 3.4. The *restriction* of a differential invariant K of order n to a curve C is the map $K|_C : C \rightarrow \mathbb{C}^2$ given by $K|_C = K \circ j_C^n$.

The coordinates of the n -th jet map j_C^n are rational functions of x and y that can be computed via implicit differentiation:

$$y_C^{(1)} = \frac{-\partial_x F}{\partial_y F} \quad \text{and} \quad y_C^{(k+1)} = \partial_x y_C^{(k)} + \partial_y y_C^{(k)} y_C^{(1)}. \quad (4)$$

where $\bar{I}_C = \langle F \rangle$. Thus, if K is a *rational* differential invariant of order n , meaning it is a rational function in the coordinates of J^n , then $K|_C$ is a rational function in x and y .

Definition 3.5. We say that a set of differential invariants \mathcal{I} *separates orbits* for the prolonged action on a nonempty Zariski-open $W \subset J^n$ if, for all $p, q \in W$,

$$K(p) = K(q) \quad \forall K \in \mathcal{I} \quad \Leftrightarrow \quad \exists g \in G \text{ such that } p = g \cdot q.$$

Definition 3.6. Let an r -dimensional algebraic group G act on \mathbb{C}^2 . A pair of rational differential invariants $\mathcal{I} = \{K_1, K_2\}$ is said to be *classifying* if K_1 separates orbits on $U_k \subset J^k$ for some $k < r$ and \mathcal{I} separates orbits on $U_r \subset J^r$.

For a particular action of G , such a pair of classifying invariants always exists, and one can explicitly construct a pair by computing generators for the field of rational invariants for the prolonged action of G [22, Thm 2.20], using algorithms such as those found in [9] and [20]. It should be noted that \mathcal{I} is not unique, and different choices can lead to different differential signatures.

Definition 3.7. For a pair of classifying invariants $\mathcal{I} = \{K_1, K_2\}$, an algebraic curve C is said to be *non-exceptional* if all but finitely many points on $p \in C$ satisfy

$$j_C^k(p) \in U_k, \quad j_C^r(p) \in U_r, \quad \text{and} \quad \frac{\partial K_1}{\partial y^{(k)}}, \frac{\partial K_2}{\partial y^{(r)}} \neq 0 \text{ at } j_C^r(p).$$

A generic curve of degree d where $\binom{d+2}{2} - 2 \geq r$ is non-exceptional with respect to a given classifying set [22, Thm 2.27].

Definition 3.8. Let $\mathcal{I} = \{K_1, K_2\}$ be a pair of classifying invariants for the action of G on \mathbb{C}^2 and C a non-exceptional algebraic curve with respect to \mathcal{I} . Then the image of C under the map

$$(K_1|_C, K_2|_C) : C \rightarrow \mathbb{C}^2$$

is the *differential signature* of C and is denoted \mathcal{S}_C .

The following appears as Theorem 2.37 in [22].

THEOREM 3.9. *If algebraic curves C_0, C_1 are non-exceptional with respect to a classifying set of rational differential invariants $\mathcal{I} = \{K_1, K_2\}$ under an action of G on \mathbb{C}^2 then*

$$C_0 \cong_G C_1 \quad \Leftrightarrow \quad \overline{\mathcal{S}_{C_0}} = \overline{\mathcal{S}_{C_1}}.$$

Example 3.10. Consider the action of the Euclidean group \mathcal{E}_2 of complex translations, rotations, and reflections on \mathbb{C}^2 where the action of $g \in \mathcal{E}_2(\mathbb{C})$ is given by

$$g \cdot (x, y) = (cx + sy + a, -sx + cy + b) \text{ or } g \cdot (x, y) = (-cx + sy + a, sx + cy + b),$$

where $c^2 + s^2 = 1$ and $c, s, a, b \in \mathbb{C}$. The pair $\mathcal{I} = \{K_1, K_2\}$ defined below is derived from classical Euclidean curvature and is classifying for the action of \mathcal{E}_2 . Here $y^{(1)} = y_x$, $y^{(2)} = y_{xx}$, and $y^{(3)} = y_{xxx}$:

$$K_1 = \frac{y_{xx}^2}{(1 + y_x^2)^3}, \quad K_2 = \frac{(y_{xxx}(1 + y_x^2) - 3y_x y_{xx}^2)}{(1 + y_x^2)^6} \quad (5)$$

Moreover, there are no I -exceptional algebraic curves—for details see [31]. By Theorem 3.9, the equivalence class of an algebraic curve C under $\mathcal{E}_2(\mathbb{C})$ is determined by \mathcal{S}_C .

3.2 Joint signatures

In [30], the author considers the use of *joint* differential signatures to determine equivalence. As an example, for the action of G on \mathbb{C}^2 given by $g \cdot (x, y) = (\bar{x}, \bar{y})$, consider the induced action on the Cartesian product space $(\mathbb{C}^2)^n = \mathbb{C}^2 \times \mathbb{C}^2 \times \dots \times \mathbb{C}^2$ given by

$$g \cdot (x_1, y_1, x_2, y_2, \dots, x_n, y_n) = (\bar{x}_1, \bar{y}_1, \bar{x}_2, \bar{y}_2, \dots, \bar{x}_n, \bar{y}_n)$$

where $\bar{x}_i = \bar{x}|_{x=x_i, y=y_i}$ and $\bar{y}_i = \bar{y}|_{x=x_i, y=y_i}$. For a curve $C \subset \mathbb{C}^2$ denote the Cartesian product by $C^n = C \times C \times \dots \times C \subset (\mathbb{C}^2)^n$. Then we can see that two curves C_0 and C_1 are G -equivalent if and only if their Cartesian products C_0^n, C_1^n are G -equivalent under the induced action on $(\mathbb{C}^2)^n$.

The advantage of considering G -equivalence of products of the curve C is that the order of the differential invariants needed to define a differential signature on this space can be reduced. Though the number of invariants required may increase, the lower order of the differential invariants can result in a more noise-resistant differential signature. In fact, for a large enough product space, it is often possible to construct a differential signature from ‘0-th order’ differential invariants, or *joint invariants*, which we refer to as a *joint signature*.

Consider the action of $\mathcal{E}_2(\mathbb{C})$ on \mathbb{C}^2 as defined in Example 3.10. This induces an action on the product space $(\mathbb{C}^2)^n$ whose joint invariants for this action are the squared inter-point distance functions

$$d_{jk}(x_j, y_j, x_k, y_k) = (x_j - x_k)^2 + (y_j - y_k)^2,$$

where $j < k$ and $j, k \in \{1, \dots, n\}$. Let the map $d_n : C^n \rightarrow \mathbb{C}^{n(n-1)/2}$ be the map which takes an n -tuple of points on C and outputs all the inter-point distances, i.e.

$$(x_1, y_1, \dots, x_n, y_n) \mapsto (d_{12}, d_{13}, \dots, d_{1n}, \dots, d_{(n-1)n}). \quad (6)$$

Additionally let W_n be the Zariski-open subset of $(\mathbb{C}^2)^n$ where all the inter-point distances do not vanish:

$$W_n = \{p \in (\mathbb{C}^2)^n \mid d_{jk}(p) \neq 0 \text{ for } j < k \text{ and } j, k \in \{1, \dots, n\}\},$$

with the convention that $W_1 = \mathbb{C}^2$. To define a joint signature for curves under $\mathcal{E}_2(\mathbb{C})$, we take $n = 4$ and follow a similar construction as the joint signature of smooth curves in \mathbb{R}^2 under the action of $\mathcal{E}_2(\mathbb{R})$ (see [30, Ex. 8.2]).

Definition 3.11. The *Euclidean joint signature* of an algebraic curve $C \subset \mathbb{C}^2$ under the action of $\mathcal{E}_2(\mathbb{C})$, which we denote \mathcal{J}_C , is the image of the polynomial map $d_4 : C^4 \rightarrow \mathbb{C}^6$ defined as in (6).

We first show that these invariant functions characterize almost all orbits of the action of $\mathcal{E}_2(\mathbb{C})$ on $(\mathbb{C}^2)^3$ and $(\mathbb{C}^2)^4$.

PROPOSITION 3.12. *The polynomial invariants $\mathcal{I}_3 = \{d_{12}, d_{13}, d_{23}\}$ separates orbits on W_3 for the induced action of \mathcal{E}_2 on $(\mathbb{C}^2)^3$ and the set*

$$\mathcal{I}_4 = \{d_{12}, d_{13}, d_{23}, d_{14}, d_{24}, d_{34}\}$$

separates orbits in W_4 for the induced action of $\mathcal{E}_2(\mathbb{C})$ on $(\mathbb{C}^2)^4$.

PROOF. Consider two triples of points $p = (p_i)_{i=1}^3$ and $q = (q_i)_{i=1}^3 \in (\mathbb{C}^2)^3$, where $p_i = (x_i^p, y_i^p)$ and q_i is denoted similarly, that take the same values on \mathcal{I}_3 and lie in W_3 . Note that W_3 excludes isotropic triples such as $(0, 0), (1, i), (1, -i)$. We will show that both triples of points necessarily lie in the same orbit. Since $d_{12} \neq 0$ we can choose a representative from the orbit of p under \mathcal{E}_2 such that $p_1 = (0, 0)$ and $p_2 = (0, y_2^p)$ by applying the transformation in $\mathcal{E}_2(\mathbb{C})$ given by

$$c = \frac{y_2^p - y_1^p}{\sqrt{d_{12}}}, s = \frac{x_2^p - x_1^p}{\sqrt{d_{12}}}, a = -x_1^p, b = -y_1^p, \quad (7)$$

and similarly we can assume for q that $q_1 = (0, 0)$ and $q_2 = (0, y_2^q)$. Since $p, q \in W_3$, $y_2^p, y_2^q \neq 0$. Thus $d_{12}(p) = d_{12}(q)$ gives that $(y_2^p)^2 = (y_2^q)^2$ meaning $y_2^p = \pm y_2^q$. Therefore, by reflecting about x -axis if necessary, we can assume $y_2^p = y_2^q$. The equations $d_{13}(p) = d_{13}(q)$ and $d_{23}(p) = d_{23}(q)$ give

$$\begin{aligned} (x_3^p)^2 + (y_3^p)^2 &= (x_3^q)^2 + (y_3^q)^2 \\ (x_3^p)^2 + (y_2^p - y_3^p)^2 &= (x_3^q)^2 + (y_2^q - y_3^q)^2. \end{aligned}$$

Subtracting these yields $(y_2^p)^2 - 2y_2^p y_3^p = (y_2^q)^2 - 2y_2^q y_3^q$ which implies $y_3^p = y_3^q$. Thus, from $d_{13}(p) = d_{13}(q)$, we have $(x_3^p)^2 = (x_3^q)^2$. From this we conclude, reflecting about the y -axis if necessary, that $x_3^p = x_3^q$. We have now shown that p and q are in the same orbit.

Suppose we have two 4-tuples of points $p = (p_i)_{i=1}^4$ and $q = (q_i)_{i=1}^4 \in (\mathbb{C}^2)^4$ that take the same values on \mathcal{I}_4 and lie in W_4 . By the previous argument we can assume that p_1, p_2 have the same form as above and that $p_i = q_i$ for $i = 1, 2, 3$. As before the equations $d_{14}(p) = d_{14}(q)$ and $d_{24}(p) = d_{24}(q)$ imply that $y_4^q = y_4^p$ and $x_4^p = \pm x_4^q$. If $x_4^p = -x_4^q$ and $x_3^p, x_3^q = 0$, then a reflection about the y -axis preserves the other values in q and sends x_4^q to $-x_4^q$. Otherwise subtracting the equations $d_{14}(p) = d_{14}(q)$ and $d_{34}(p) = d_{34}(q)$ yields $-2x_3^p x_4^p = -2x_3^q x_4^q$, which implies that $x_4^p = x_4^q$. Thus p and q must lie in the same orbit. \square

LEMMA 3.13. *For an algebraic curve $C \subset \mathbb{C}^2$ and $n > 1$, a generic n -tuple of points on C^n lies inside W_n . Additionally for any fixed $(n-1)$ -tuple of points in $(p_1, \dots, p_{n-1}) \in W_{n-1} \cap C^{n-1}$ and a generic point $p_n \in C$, the n -tuple (p_1, \dots, p_n) lies in W_n .*

PROOF. For $n = 2$, fix any $p_1 = (x_1, y_1) \in C$. If $d_{1,2} = 0$ for all $(x_2, y_2) \in C$, then C must lie in a union of lines defined by

$$\{(x_2, y_2) \in \mathbb{C}^2 \mid (x_1 - x_2 + y_1 - y_2)(x_1 - x_2 - iy_1 + iy_2) = 0\}.$$

Since C is irreducible, this contradicts $\deg(C) > 1$. Thus the set $U_{2,p_1} = \{p_2 \in C \mid d_{1,2} \neq 0\}$, which is Zariski-open in C , is also nonempty. Thus, for any particular $p_1 \in C$, there exists p_2 with $(p_1, p_2) \in W_2 \cap C^2$, from which both claims follow. Inductively, we fix any $(p_1, \dots, p_{n-1}) \in W_{n-1} \cap C^{n-1}$. As before, the sets

$$U_{i,p_1,\dots,p_{n-1}} = \{p_n \in C \mid d_{in} \neq 0\}$$

are open and nonempty. Thus a generic $p_n \in C$ lies in their intersection, and hence $(p_1, \dots, p_n) \in W_n$. \square

PROPOSITION 3.14. *The stabilizer of $p \in W_2$ or $p \in W_3$ under the action of $\mathcal{E}_2(\mathbb{C})$ is a finite subgroup.*

PROOF. The stabilizer of a point $p \in (\mathbb{C}^2)^2$ is the subgroup of $\mathcal{E}_2(\mathbb{C})$ given by

$$\mathcal{E}_2(\mathbb{C})_p = \{g \in \mathcal{E}_2(\mathbb{C}) \mid g \cdot p = p\}.$$

The size of the stabilizer of a point is preserved by the action of the group. Since $d_{12}(p) \neq 0$, by applying the transformation in (7), we can assume p has the form $p = (p_1, p_2) = (0, 0, 0, y_2)$ where $y_2 \neq 0$. Given the parameterization of $\mathcal{E}_2(\mathbb{C})$ in Example 3.10, $g \cdot p = p$ immediately implies that $a = b = 0$ and that $sy_2 = 0$. Thus $\mathcal{E}_2(\mathbb{C})_p$ consists of either the identity transformation or a reflection about the y -axis. The same result immediately follows for $p \in W_3$, since $(p_1, p_2, p_3) \in W_3$ implies that $(p_1, p_2) \in W_2$. \square

LEMMA 3.15. *For plane curves C_0, C_1 , suppose that there exists $p = (p_1, p_2) \in C_0^2, C_1^2$ such that $p \in W_2$ and*

$$d_3(p_1 \times p_2 \times C_0) = d_3(p_1 \times p_2 \times C_1).$$

Then there exists $g \in \mathcal{E}_2(\mathbb{C})$ such that $g \cdot C_0 = C_1$.

PROOF. By Lemma 3.13, for a generic point $q \in C_0$, the 3-tuple $(p_1, p_2, q) \in W_3$. Since both curves have the same image under d_3 , there exists a point $r \in C_1$ such that $r \in d_3^{-1}(p_1, p_2, q)$. By Proposition 3.12, both triples (p_1, p_2, q) and (p_1, p_2, r) lie in the same orbit under $\mathcal{E}_2(\mathbb{C})$, and hence there exists $g \in \mathcal{E}_2(\mathbb{C})$ such that $g \cdot (p_1, p_2, q) = (p_1, p_2, r)$. However, this implies that $g \in \mathcal{E}_2(\mathbb{C})_{(p_1, p_2)}$. By Proposition 3.14, $\mathcal{E}_2(\mathbb{C})_{(p_1, p_2)} = \{e, h\}$ where $h \in \mathcal{E}_2(\mathbb{C})$ is a reflection about the line containing p_1 and p_2 . Therefore $q = r$ or $h \cdot q = r$, implying that C_1 shares infinitely many points with C_0 or $h \cdot C_0$, proving the lemma. \square

LEMMA 3.16. *For plane curves C_0, C_1 , suppose that there exists a 3-tuple $p = (p_1, p_2, p_3) \in C_0^3, C_1^3$ such that $p \in W_3$ and*

$$d_4(p_1 \times p_2 \times p_3 \times C_0) = d_4(p_1 \times p_2 \times p_3 \times C_1).$$

Then there exists $g \in \mathcal{E}_2(\mathbb{C})$ such that $g \cdot C_0 = C_1$.

PROOF. The proof follows similarly as in Lemma 3.15 by applying Propositions 3.12 and 3.14. \square

PROPOSITION 3.17. *Two plane curves $C_0, C_1 \subset \mathbb{C}^2$ of degree $d > 2$ are $\mathcal{E}_2(\mathbb{C})$ -equivalent if and only if $\overline{\mathcal{I}_{C_0}} = \overline{\mathcal{I}_{C_1}}$.*

PROOF. Since the map $d_i : C_i^4 \rightarrow \mathbb{C}^6$ for $i = 0, 1$ is defined by $\mathcal{E}_2(\mathbb{C})$ -invariants the forward direction is clear. For the remainder of the proof assume that $\overline{\mathcal{I}_{C_0}} = \overline{\mathcal{I}_{C_1}} := \mathcal{J}$. We deal with two cases. Either the image of the map $d_3 : C_0^3 \rightarrow \mathbb{C}^3$ lies in a Zariski-closed subset of dimension ≤ 2 or is Zariski-dense in \mathbb{C}^3 .

First suppose that $d_3(C_0^3)$ (and hence $d_3(C_1^3)$) is Zariski-dense in \mathbb{C}^3 . This implies $\dim(\mathcal{J})$ equals 3 or 4. Consider the projection $\pi_{12} : \mathcal{J} \rightarrow \mathbb{C}$ of \mathcal{J} onto the first coordinate d_{12} . Let $\mathcal{H}_{12} = \pi_{12}^{(-1)}(r)$ be the pullback of a generic point so that $\dim(\mathcal{H}_{12} \cap \mathcal{J})$ equals 2 or 3. Appealing to Bertini's Theorem as in Proposition 2.3, the singular points of $\mathcal{H}_{12} \cap \mathcal{J}$ are also singular points of \mathcal{J} . For similarly defined \mathcal{H}_{13} and \mathcal{H}_{23} let $\mathcal{Y} = \mathcal{H}_{12} \cap \mathcal{H}_{13} \cap \mathcal{H}_{23} \cap \mathcal{J}$. Then $\dim(\mathcal{Y})$ equals 0 or 1, and the singular points of \mathcal{Y} are singular points of \mathcal{J} .

Consider a generic 4-tuple of points $p = (p_1, p_2, p_3, p_4) \in C_0^4$. Since the $d_4(C_i)$ agree on a dense set, we may assume $d_4(p) \in d_4(C_0) \cap d_4(C_1)$. Taking generic $\mathcal{H}_{12} \cap \mathcal{H}_{13} \cap \mathcal{H}_{23}$ through $d_3(p)$ and \mathcal{Y} as in the previous paragraph, we have that $d_4(p)$ is a non-singular point of \mathcal{Y} . Let $q = (q_1, q_2, q_3, q_4)$ be a point on C_1^4 in

the inverse image $d_4^{-1}(d_4(p))$. By Proposition 3.12 and Lemma 3.13, there exists some $g \in \mathcal{E}_2(\mathbb{C})$ such that $g \cdot q = p$. Let $C_2 = g \cdot C_1$.

Note that $\dim(d_4(p_1 \times p_2 \times p_3 \times C_0)) = 0$ implies that the function $d_{14}(x) = d_{14}(p_1, p_2, p_3, x)$ is constant on C_0 , and similarly so are $d_{24}(x)$ and $d_{34}(x)$. By Proposition 3.12, for a generic point $x \in C_0$, the 4-tuples (p_1, p_2, p_3, x) are all related by an element of $\mathcal{E}_2(\mathbb{C})$. However this is a contradiction, since by Proposition 3.14 there are finitely many such elements. Thus both $d_4(p_1 \times p_2 \times p_3 \times C_0)$ and similarly $d_4(p_1 \times p_2 \times p_3 \times C_1)$ are dimension 1 lying in \mathcal{Y} . Since $\dim(\mathcal{Y}) = 1$ there are both dense in some irreducible component of \mathcal{Y} . Since $d_4(p)$ is a non-singular point of \mathcal{Y} , it is necessarily contained in exactly one irreducible component of \mathcal{Y} . Therefore

$$d_4(p_1 \times p_2 \times p_3 \times C_0) = d_4(p_1 \times p_2 \times p_3 \times C_2).$$

By Lemma 3.16, $C_0 = C_2 = g \cdot C_1$, completing the proof for the case where $d_3(C_0^3) \subset \mathbb{C}^3$ is Zariski dense. The remaining case follows analogously (take $\mathcal{Y} = \mathcal{H}_{12} \cap d_3(C_0^3)$ and apply Lemma 3.15). \square

4 IMPLEMENTATION, EXAMPLES, AND EXPERIMENTS

Our implementation of Algorithm 1 treats only the special case where the domain of each rational map is some Cartesian product of irreducible plane curves, say $X_i = C_i^k$ for some integer k . Our results showcase features of the NumericalAlgebraicGeometry ecosystem in Macaulay2 (aka NAG4M2, see [23, 24] for an overview.) We rely extensively on the core path-tracker and the packages SLPexpressions and MonodromySolver. All of our examples and experiments deal with differential and joint signatures for the Euclidean group.² However, the current functionality should make it easy to study other group actions and variations on the signature construction in the future.

For the purpose of our implementation, the various ingredients for the input to Algorithm 1 are easily provided. Suppose $\mathcal{I}_{C_i} = \langle f_i \rangle$ for $i = 0, 1$. Then the reduced regular sequence we need is given by $(f_0(x_1, y_1), \dots, f_0(x_k, y_k))$. Sampling from X_0 amounts to sampling k times from C_0 ; we sample the curve C_0 using homotopy continuation from a linear-product start system [33, 8.4.3]. Finally, a witness set for the image of the signature map Φ_1 can be computed using methods of numerical algebraic geometry. Heuristics based on *monodromy* allow us to make this offline computation relatively efficient; MonodromySolver implements a general framework described in [5, 10]. We also observe that a witness set for the signature of a particular curve may be computed if we have already computed a witness set for the corresponding signature of some *generic* curve of the same degree. This is yet another application of coefficient parameter homotopy. [27] The efficiency of these two methods is compared in Example 4.1.

We explain some aspects of our implementation that appear to give reasonable numerical stability. A key feature is that polynomials and rational maps are given by straight-line programs as opposed to their coefficient representations. This is especially crucial in the case of differential signatures, where we can do efficient evaluation using the formulas in equation 4; we note that expanding these rational functions in the monomial basis involves many terms

²For details we refer to the code: <https://github.com/timduff35/NumericalSignatures>.

d	$\deg S$	time (s)	$\deg_{(1,0)} S$	time (s)
2	6	0.3	3	0.1
3	72	2	36	0.5
4	144	9	72	2
5	240	21	120	4
6	360	55	180	7

Figure 2: Degrees and monodromy timings for differential signatures.

d	$\deg \mathcal{J}$	time (s)	$\deg_{e_1} \mathcal{J}$	time (s)	$\deg_{e_2} \mathcal{J}$	time (s)
2	42	4	24	2	26	2
3	936	33	576	17	696	16
4	3024	139	1920	57	2448	87
5	7440	463	4800	206	6320	276
6	15480	1315	10080	748	13560	791

Figure 3: Degrees and monodromy timings for joint signatures (see Conjecture 4.2.)

and does not suggest a natural evaluation scheme. We also homogenize the equations of our plane curves and work in a random affine chart. Finally, in our sampling procedure we discard samples which map too close to the origin in the codomain of our maps, as these tend to produce nearly-singular points on the image.

Example 4.1. The code below computes a witness set for the differential signature of a “generic” quartic (whose coefficients are random complex numbers of modulus 1.)

```
(d, k) = (4, 1);
dom = domain(d, k);
Map = diffEuclideanSigMap dom;
H = witnessHomotopy(dom, Map);
W = runMonodromy H;
```

To compute a witness set for the differential signature of the Fermat quartic $V(x^4 + y^4 + z^4) \subset \mathbb{P}(\mathbb{C}^3)$, we use the previous computation.

```
R = QQ[x, y, z];
f = x^4 + y^4 + z^4;
Wf = witnessCollect(f, W)
```

The output resulting from the last line reads

witness data w/ 18 image points (144 preimage points) indicating that the differential signature map is generically 8 to 1, which is equivalent to the Fermat curve having eight Euclidean symmetries [22, Thm 2.38]. We timed these witness set computations at 5 and 0.5 seconds, respectively. For joint signatures, the analogous computations were timed at 95 and 17 seconds.

Figures 2 and 3 give degrees and single-run timings for monodromy computations on curves up to degree 6. We also considered multiprojective witness sets for $S \subset \mathbb{C}^1 \times \mathbb{C}^1$ and $\mathcal{J} \subset (\mathbb{C}^1)^6$, where fewer witness points are needed. For the differential signatures, we considered $(1, 0)$ -slices which fix the value of K_1 in (5). For joint signatures, there are two combinatorially distinct classes of $(\mathbb{C}^1)^6$ witness sets determined by which $d_{i,j}$ are fixed; the undirected graph of fixed distances must either be the 3-pan (a 3-cycle with

d	track time (ms)	lookup time (ms)	track K_1	lookup K_1
2	191	0.35	127	0.25
3	177	0.37	121	0.31
4	276	0.42	145	0.36
5	472	0.39	203	0.43
6	597	0.40	284	0.37

Figure 4: Equality test timings for differential signatures S_d .

d	track time (ms)	lookup time (ms)	track e_1	lookup e_1
2	230	0.36	208	0.34
3	283	0.38	213	0.35
4	335	0.39	288	0.40
5	409	0.32	357	0.32
6	507	0.32	462	0.33

Figure 5: Equality test timings for joint signatures \mathcal{J}_d .

pendant edge) or the 4-cycle. We fix corresponding multidimensions $e_1 = (1, 1, 1, 1, 0, 0)$ and $e_2 = (0, 1, 1, 1, 1, 0)$.

The timings in figures 2 and 3 are not optimal for a number of reasons. For instance, some multiprojective witness sets have an *imprimitive* monodromy action, meaning that additional symmetries can be exploited [2]. We successfully ran monodromy (with less conservative settings) for both signature maps on curves of degree up to 10. These computations suggested formulas for the degrees. For the joint signature, we state these formulas in the form of a conjecture. For the case of differential signatures, see [22]; degrees for $d = 2$ are corrected by a factor of 4.

CONJECTURE 4.2. Let \mathcal{J}_d denote the joint signature for a generic plane curve of degree d . For $d \geq 3$:

$$\begin{aligned} \deg \mathcal{J}_d &= 12d(d^3 - 1) \\ \deg_{e_1} \mathcal{J}_d &= 8d^2(d^2 - 1) \\ \deg_{e_2} \mathcal{J}_d &= 4d(d - 1)(3d^2 + d - 1). \end{aligned}$$

To assess the speed and robustness of the online equality test, we conducted an experiment where, for degrees $d = 2, \dots, 6$, curves C_1, \dots, C_{10} were generated with coefficients drawn uniformly from the unit sphere in $\mathbb{R}^{(d+2)(d+1)/2}$. For each C_i , we computed a witness set via parameter homotopy from a generic degree d curve. We then applied 20 random transformations from $\mathcal{E}_2(\mathbb{R})$ to the C_i and perturbed the resulting coefficients by random real $\tilde{\epsilon}$ with $\|\tilde{\epsilon}\|_2 \in \{0, 10^{-7}, 10^{-6}, \dots, 10^{-3}\}$, thus obtaining curves $\widetilde{C_{i,1,\epsilon}}, \dots, \widetilde{C_{i,20,\epsilon}}$. With all numerical tolerances fixed, we ran the equality test for each $\widetilde{C_{i,j,\epsilon}}$ against each C_i .

Figures 4 and 5 summarize the timings for the equality tests in this experiment. Overall, these tests run on the order of sub-seconds. Most of the time is spent on path-tracking. The tracking times reported give the total time spent on lines 1 and 5 of Algorithm 1. The only other possible bottleneck is the lookup on line 7. This is negligible, even for large witness set sizes, if an appropriate data structure is used. The runtimes for all cases considered seem comparable, although using differential signatures and multiprojective slices appear to give a slight edge over the respective alternatives.

The plots in Figure 6 illustrate the results of our sensitivity analysis. The respective axes are the magnitude of the noise ϵ and

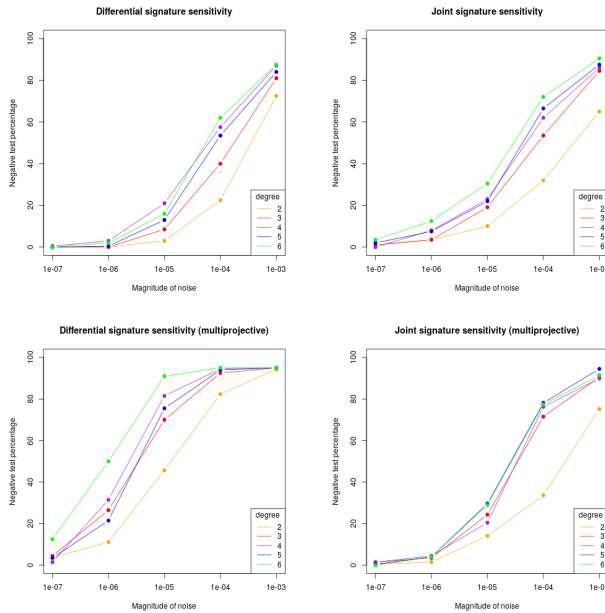


Figure 6: Sensitivity of the equality test to noise.

the percentage of $C_{i,j,\epsilon}$ deemed to be not equivalent to C_i . Note that the horizontal axis is given on a log scale, and excludes the noiseless case $\epsilon = 0$; for this case, among all tests in the experiment, only one false negative was reported for the differential signatures with $d = 6$. We include a trend line to make the plots more readable. In general, we observe a threshold phenomenon, where most tests are positive for sufficiently low noise and are negative for sufficiently high noise.

The thresholds displayed in Figure 6 clearly depend on the numerical tolerances used (for this experiment, defaults provided by NAG4M2), the type of map, and the type of witness set. Besides the multiprojective differential signature (depicted in the bottom-left), we observe a similar stability profile for this type of random perturbation. We speculate that similar analyses, based on a more meaningful model of noise, may highlight further differences between the joint and differential signatures.

ACKNOWLEDGMENTS

Research of T. Duff is supported in part by NSF DMS-1719968, a fellowship from the Algorithms and Randomness Center at Georgia Tech, and by the Max Planck Institute for Mathematics in the Sciences in Leipzig.

REFERENCES

- [1] E. L. Allgower and K. Georg. 2012. *Numerical continuation methods: an introduction*. Vol. 13. Springer Science & Business Media.
- [2] C. Améndola and J. I. Rodríguez. 2016. Solving parameterized polynomial systems with decomposable projections. *arXiv preprint arXiv:1612.08807* (2016).
- [3] D. J. Bates, A. J. Hauenstein, Jonathan D Sommese, and C. W. Wampler. 2013. *Numerically solving polynomial systems with Bertini*. SIAM.
- [4] I. A. Berchenko (Kogan) and P. J. Olver. 2000. Symmetries of Polynomials. *Journal of Symbolic Computations* 29 (2000), 485–514.
- [5] N. Bliss, T. Duff, A. Leykin, and J. Sommars. 2018. Monodromy solver: sequential and parallel. In *Proceedings of the 2018 ACM International Symposium on Symbolic and Algebraic Computation*. 87–94.

- [6] T. Brysiewicz. 2018. Numerical Software to Compute Newton Polytopes. In *International Congress on Mathematical Software*. Springer, 80–88.
- [7] J. M. Burdis, I. A. Kogan, and H. Hong. 2013. Object-image correspondence for algebraic curves under projections. *SIGMA Symmetry Integrability Geom. Methods Appl.* 9 (2013), Paper 023, 31.
- [8] J. Chen and J. Kileel. 2019. Numerical implicitization for Macaulay2. *Journal of Software for Algebra and Geometry* 9 (2019), 55–65.
- [9] H. Derksen and G. Kemper. 2015. *Computational invariant theory* (enlarged ed.). Encyclopaedia of Mathematical Sciences, Vol. 130. Springer, Heidelberg. xxii+366 pages.
- [10] T. Duff, C. Hill, A. Jensen, K. Lee, A. Leykin, and J. Sommars. 2019. Solving polynomial systems via homotopy continuation and monodromy. *IMA J. Numer. Anal.* 39, 3 (2019), 1421–1446.
- [11] M. Fels and P. J. Olver. 1999. Moving Coframes. II. Regularization and Theoretical Foundations. *Acta Appl. Math.* 55 (1999), 127–208.
- [12] D. Grayson and M. Stillman. 1997. Macaulay 2—a system for computation in algebraic geometry and commutative algebra.
- [13] A. Grim and C. Shakiban. 2017. Applications of signature curves to characterize melanomas and moles. In *Applications of computer algebra*. Springer Proc. Math. Stat., Vol. 198. Springer, Cham, 171–189.
- [14] J. Harris. 2013. *Algebraic geometry: a first course*. Vol. 133. Springer Science & Business Media.
- [15] J. D. Hauenstein, A. Leykin, J. I. Rodríguez, and F. Sottile. 2019. A numerical toolkit for multiprojective varieties. *arXiv preprint arXiv:1908.00899* (2019).
- [16] J. D. Hauenstein and J. I. Rodríguez. 2019. Multiprojective witness sets and a trace test. *To appear in Advances in Geometry*. *arXiv preprint arXiv:1507.07069* (2019).
- [17] J. D. Hauenstein and A. J. Sommese. 2010. Witness sets of projections. *Appl. Math. Comput.* 217, 7 (2010), 3349–3354.
- [18] J. D. Hauenstein and A. J. Sommese. 2013. Membership tests for images of algebraic sets by linear projections. *Appl. Math. Comput.* 219, 12 (2013), 6809–6818.
- [19] D. J. Hoff and P. J. Olver. 2014. Automatic solution of jigsaw puzzles. *J. Math. Imaging Vision* 49, 1 (2014), 234–250.
- [20] E. Hubert and I. A. Kogan. 2007. Smooth and algebraic invariants of a group action: local and global construction. *Foundation of Computational Math.* 7:4 (2007), 345–383.
- [21] I. A. Kogan and M. Moreno Maza. 2002. Computation of canonical forms for ternary cubics. In *Proceedings of the 2002 International Symposium on Symbolic and Algebraic Computation*. ACM, New York, 151–160.
- [22] I. A. Kogan, M. Ruddy, and C. Vinzant. 2020. Differential Signatures of Algebraic Curves. *SIAM J. Appl. Algebra Geom.* 4, 1 (2020), 185–226.
- [23] A. Leykin. 2011. Numerical algebraic geometry. *Journal of Software for Algebra and Geometry* 3, 1 (2011), 5–10.
- [24] A. Leykin. 2018. Homotopy Continuation in Macaulay2. In *International Congress on Mathematical Software*. Springer, 328–334.
- [25] A. Leykin, J. I. Rodríguez, and F. Sottile. 2018. Trace test. *Arnold Mathematical Journal* 4, 1 (2018), 113–125.
- [26] A. Morgan. 2009. *Solving polynomial systems using continuation for engineering and scientific problems*. Vol. 57. SIAM.
- [27] A. P. Morgan and A. J. Sommese. 1989. Coefficient-parameter polynomial continuation. *Appl. Math. Comput.* 29, 2 (1989), 123–160.
- [28] P. J. Olver. 1995. *Equivalence, invariants and symmetry*. Cambridge University Press.
- [29] P. J. Olver. 1999. *Classical invariant theory*. London Mathematical Society Student Texts, Vol. 44. Cambridge University Press, Cambridge. xxii+280 pages.
- [30] P. J. Olver. 2001. Joint invariant signatures. *Found. Comput. Math.* 1, 1 (2001), 3–67.
- [31] M. Ruddy. 2019. *The Equivalence Problem and Signatures of Algebraic Curves*. Ph.D. Dissertation. North Carolina State University.
- [32] A. J. Sommese, J. Verschelde, and C. W. Wampler. 2005. Introduction to numerical algebraic geometry. In *Solving polynomial equations*. Springer, 301–337.
- [33] I. C. W. Wampler et al. 2005. *The Numerical solution of systems of polynomials arising in engineering and science*. World Scientific.